NASA/ TM—1998-207922 AIAA–98–2289

# On the Role of Anisotropy in Turbulent Mixing Noise

A. Khavaran
NYMA, Inc., Brook Park, Ohio

E.A. Krejsa
Lewis Research Center, Cleveland, Ohio

May 1998

## The NASA STI Program Office . . . in Profile

Since its founding, NASA has been dedicated to the advancement of aeronautics and space science. The NASA Scientific and Technical Information (STI) Program Office plays a key part in helping NASA maintain this important role.

The NASA STI Program Office is operated by Langley Research Center, the Lead Center for NASA's scientific and technical information. The NASA STI Program Office provides access to the NASA STI Database, the largest collection of aeronautical and space science STI in the world. The Program Office is also NASA's institutional mechanism for disseminating the results of its research and development activities. These results are published by NASA in the NASA STI Report Series, which includes the following report types:

- TECHNICAL PUBLICATION. Reports of completed research or a major significant phase of research that present the results of NASA programs and include extensive data or theoretical analysis. Includes compilations of significant scientific and technical data and information deemed to be of continuing reference value. NASA's counterpart of peer-reviewed formal professional papers but has less stringent limitations on manuscript length and extent of graphic presentations.

- TECHNICAL MEMORANDUM. Scientific and technical findings that are preliminary or of specialized interest, e.g., quick release reports, working papers, and bibliographies that contain minimal annotation. Does not contain extensive analysis.

- CONTRACTOR REPORT. Scientific and technical findings by NASA-sponsored contractors and grantees.

- CONFERENCE PUBLICATION. Collected papers from scientific and technical conferences, symposia, seminars, or other meetings sponsored or cosponsored by NASA.

- SPECIAL PUBLICATION. Scientific, technical, or historical information from NASA programs, projects, and missions, often concerned with subjects having substantial public interest.

- TECHNICAL TRANSLATION. English-language translations of foreign scientific and technical material pertinent to NASA's mission.

Specialized services that complement the STI Program Office's diverse offerings include creating custom thesauri, building customized data bases, organizing and publishing research results . . . even providing videos.

For more information about the NASA STI Program Office, see the following:

- Access the NASA STI Program Home Page at ***http://www.sti.nasa.gov***

- E-mail your question via the Internet to help@sti.nasa.gov

- Fax your question to the NASA Access Help Desk at (301) 621-0134

- Telephone the NASA Access Help Desk at (301) 621-0390

- Write to:
  NASA Access Help Desk
  NASA Center for AeroSpace Information
  7121 Standard Drive
  Hanover, MD 21076

NASA/ TM—1998-207922 AIAA–98–2289

# On the Role of Anisotropy in Turbulent Mixing Noise

A. Khavaran
NYMA, Inc., Brook Park, Ohio

E.A. Krejsa
Lewis Research Center, Cleveland, Ohio

Prepared for the
Fourth Aeroacoustics Conference
cosponsored by the American Institute of Aeronautics and Astronautics
and the Confederation of European Aerospace Societies
Toulouse, France, June 2–4, 1998

National Aeronautics and
Space Administration

Lewis Research Center

May 1998

Available from

NASA Center for Aerospace Information
7121 Standard Drive
Hanover, MD 21076
Price Code: A03

National Technical Information Service
5287 Port Royal Road
Springfield, VA 22100
Price Code: A03

# On the Role of Anisotropy in Turbulent Mixing Noise

Abbas Khavaran
NYMA, Inc., Lewis Research Group, Cleveland, OH 44135

Eugene A. Krejsa
NASA Lewis Research Center, Cleveland, OH 44135

**Abstract**

This paper investigates the effect of anisotropy on aerodynamic mixing noise due to a fine-scale turbulence. The usual assumption of isotropic turbulence is replaced with that of an axisymmetric turbulence. The analysis is based on source terms of Lilley's equation. In addition, acoustic-flow interaction is accounted for in terms of a high-frequency solution to the axisymmetric Lilley's equation. In the limiting case of isotropy, various source correlation terms derived here will simplify to those obtained with an isotropic turbulence model. A Reynolds averaged Navier-Stokes solution with a $k$-$\epsilon$ turbulence model for a Mach 1.0 jet was used to make acoustic predictions. A parametric study of the turbulence scales indicates that anisotropy increases the peak noise level.

## 1. Introduction

Ongoing efforts at NASA-Lewis are underway to develop jet exhaust mixers that will reduce noise compared to base geometries operating under similar conditions. This effort has shown a need for more sophisticated prediction tools to address new parameters that may affect aerodynamic noise generation and propagation. To develop these tools some of the usual assumptions for modeling of sources of a fine-scale turbulence may have to be revised. An improved prediction model needs to address turbulence characteristics as observed through experiment. One class of such observations confirms the non-isotropy of turbulence. For example, measurements by Jones[1] and Bradshaw[2] at low subsonic Mach numbers of 0.1 and 0.3 and the more recent measurements by Zysman[3] and Podboy[4] for high subsonic and transonic jets confirm a high degree of anisotropy among turbulence intensity components. Figure 1 shows the measured root-mean-square of the turbulent velocities for three nozzle geometries cited in Ref. 4. These geometries are low-bypass ratio mixers operating at a pressure ratio of 1.96. Indications are that the mean flow creates a preferred direction and that turbulent intensities of $v$ and $w$ in a span-wise direction are distinctly different from that of $u$ in a stream-wise direction.



Hence, if we neglect the small difference in intensities of $v$ and $w$, clearly an axisymmetric turbulence is a natural extension beyond isotropy. In this paper, we propose an axisymmetric turbulence model, compatible with conditions of symmetry as stated in Ref. 5, and derive closed-form expressions for quadrupole sources of various orientations. The sources are associated with a fine-scale turbulence and are modeled after two-point time-delayed fourth-order space-time velocity correlations. It will be shown that the usual assumption of space and time separation is not a requirement in modeling the turbulent velocity correlations. A Reynolds averaged Navier-Stokes solution with a $k$-$\epsilon$ turbulence model will provide the mean flow and the turbulence kinetic energy. Two new parameters are addressed in connection with turbulence anisotropy. These are length scale ratio and the ratio between components of turbulence intensity in an axisymmetric turbulence. The analysis continues with modeling of the self- and shear-noise terms of Lilley's equation and inclusion of the mean flow refraction effects. Sample spectra and directivity predictions for a low-bypass ratio dual-flow coaxial jet, and role of anisotropy parameters are discussed. It is demonstrated that increasing the turbulence anisotropy will increase the overall noise level.

## 2. Source Modeling

The theory of axisymmetric turbulence was originally proposed by Batchelor[6]. Further developments in the theory, including a complete derivation of axisymmetric tensors, were worked by Chandrasekhar[5]. Here we propose a model compatible with the requirements of symmetry as stated in references 5 and 6 and derive two-point velocity correlations describing the noise sources of the fine-scale turbulence. In the limiting case, these models will simplify to that of Batchelor's[7] isotropic turbulence model; hence, velocity correlations of various orientations reduce to those of an isotropic turbulence.

We start with a fourth-order space-time velocity correlation and assume that it may be expressed in terms of second-order correlations

$$\overline{v_i v_j v'_k v'_\ell} = \overline{(v_i v_j)}\,\overline{(v'_k v'_\ell)} + \overline{(v_i v'_k)}\,\overline{(v_j v'_\ell)} + \overline{(v_i v'_\ell)}\,\overline{(v_j v'_k)}, \tag{1}$$

where $\overline{v_i v'_j}$ is the velocity correlation between two points $\vec{y}$ and $\vec{y'}$ separated by a vector $\vec{\xi}$ and a time-delay $\tau$. Let's consider a source correlation term due to a unit volume of turbulence

$$I_{ijk\ell}(\tau) = \rho^2 \int_{\vec{\xi}} \frac{\partial^4}{\partial \tau^4} \overline{v_i v_j v'_k v'_\ell} d\vec{\xi}, \tag{2}$$

for $0 \leq |\vec{\xi}| < \infty$. Substituting (1) into (2), we obtain

$$I_{ijk\ell}(\tau) = \rho^2 \frac{\partial^4}{\partial \tau^4} \int_{\vec{\xi}} [(\overline{v_i v'_k})(\overline{v_j v'_\ell}) + (\overline{v_i v'_\ell})(\overline{v_j v'_k})] d\vec{\xi}. \tag{3}$$

The corresponding noise spectra for a source of frequency $\Omega$ is the Fourier transform of the autocorrelation function

$$I_{ijk\ell}(\Omega) = \frac{1}{2\pi} \int_{-\infty}^{+\infty} I_{ijk\ell}(\tau) e^{i\Omega\tau} d\tau. \tag{4}$$

### 2.1 Isotropic Turbulence

To carry on with the integration of Eqs. (3) and (4), it is convenient to assume space and time separation as suggested by Ribner[8] and express two-point velocity correlations as

$$\overline{v_i v'_j} = R_{ij}(\vec{\xi}) g(\tau). \tag{5}$$

In section 2.3, we argue that separability is not a requirement in modeling two-point correlation functions and non-separable expressions may lead to identical results. For a homogeneous isotropic turbulence, the space factor $R_{ij}$ was given by Batchelor[7] as

$$R_{ij}(\vec{\xi}) = \overline{u_1^2}[(f + \frac{1}{2}\xi f')\delta_{ij} - \frac{1}{2} f' \xi_i \xi_j / \xi]. \tag{6}$$

where $\overline{u_1^2}$ represents 1/3 of the turbulence intensity and $f' = \partial f / \partial \xi$. The three components of the separation vector are represented as $\xi_i$ for $i = 1, 2, 3$. Function $f(\xi)$ may be expressed as $f(\xi) = exp(-\pi \xi^2 / L^2)$. This expression makes $f(\xi)$ decrease to zero for large $\xi$ with sufficient rapidity to make $\int_0^\infty \xi^m f(\xi) d\xi$ converge for $m \geq 0$. Length $L$ is the longitudinal integral length-scale, representing the linear extent of the region within which velocities are appreciably correlated. Substitution of (5) and (6) in (3) will give

$$I_{1111}(\tau) = \rho^2 \frac{\partial^4}{\partial \tau^4} g^2(\tau) \frac{(\overline{u_1^2})^2 L^3}{2\sqrt{2}}, \tag{7}$$

$$I_{2222} = I_{3333} = I_{1111},$$

$$I_{1122} = I_{1133} = I_{2233} = \frac{1}{8} I_{1111},$$

$$I_{1212} = I_{1313} = I_{2323} = \frac{7}{16} I_{1111}.$$

### 2.2 Axisymmetric Turbulence

We assume that index 1 refers to a stream-wise direction that also coincides with the axis of turbulence symmetry. In a span-wise plane, turbulent velocity components for an axisymmetric turbulence are related

$$\overline{u_2^2} = \overline{u_3^2}. \tag{8}$$

Let $\beta = (1 - \overline{u_2^2}/\overline{u_1^2})$ and express the turbulence kinetic energy $k$ as

$$k = \frac{1}{2}(\overline{u_1^2} + \overline{u_2^2} + \overline{u_3^2}) = \frac{3}{2}\overline{u_1^2}(1 - \frac{2}{3}\beta). \tag{9}$$

In an axisymmetric turbulence, two-point velocity correlations are given as[5]

$$\overline{v_i v'_j} = \epsilon_{j\ell m} \frac{\partial q_{im}}{\partial \xi_\ell}, \tag{10}$$

where skew tensor $q_{im}$ is

$$q_{im} = Q_1 \epsilon_{imk} \xi_k + (Q_2 \lambda_m + Q_3 \xi_m) \epsilon_{i\ell k} \lambda_\ell \xi_k, \tag{11}$$

and scalar functions $Q_1$, $Q_2$, and $Q_3$ are functions of $|\vec{\xi}|$, $\xi_1$, $\tau$, and source location $\vec{y}$. Turbulence is assumed as locally homogeneous, and the incompressibility condition $\partial \overline{v_i v'_j} / \partial \xi_i = 0$ is identically satisfied by expression (10). Unit vector $\vec{\lambda}$ is in the direction of turbulence symmetry, and $\epsilon_{j\ell m}$ is the usual alternator. With $\vec{\lambda} = (1, 0, 0)$, Eq. (11) may be written as

$$q_{im} = \xi_k [\epsilon_{imk} Q_1 + \epsilon_{i1k}(\delta_{1m} Q_2 + \xi_m Q_3)]. \tag{12}$$

Interchangeability requires $\overline{v_i v'_j} = \overline{v_j v'_i}$, and when we use (10) and (12) it leads to the following relations between scalar functions $Q_1$, $Q_2$ and $Q_3$

$$(\xi_3 \frac{\partial}{\partial \xi_2} - \xi_2 \frac{\partial}{\partial \xi_3}) Q_i = 0, \qquad (i = 1, 2) \tag{13a}$$

$$Q_3 = (\frac{\partial}{\partial \xi_1} - \frac{\xi_1}{\xi_3} \frac{\partial}{\partial \xi_3}) Q_1. \tag{13b}$$

We propose a set of scalar functions $Q_1$ and $Q_2$ kinematically compatible with conditions (13a)

$$Q_1 = -(\frac{\overline{u_1^2}}{2}) g(\tau) e^{-\pi(\xi_1^2/L_1^2 + \xi_{23}^2/L_2^2)}, \tag{14a}$$

$$Q_2 = -(\overline{u_2^2} - \overline{u_1^2}) g(\tau) e^{-\pi(\xi_1^2/L_1^2 + \xi_{23}^2/L_2^2)}. \tag{14b}$$

Function $Q_3$ is derived from (13b). In (14), $\xi_{23}^2 = \xi_2^2 + \xi_3^2$, and $L_1$ and $L_2$ denote stream- and span-wise correlation length-scales, respectively. It is implicit that $g(\tau)$

be a function of source coordinate $\vec{y}$ . We note that the above scalar functions are different from those proposed by Goldstein[9] and used thereafter by Bechara *et al*[10]. Various two-point correlations derived from the above scalar functions are compatible with Batchelor's model as given in Eqs. (5) and (6). Moreover, the analysis allows for flow/acoustics interaction by multiplying each source correlation by its corresponding directivity factor obtained from a solution to the axisymmetric Lilley's equation. A substitution of Eq. (14) into (12) and (10) combined with (3) leads to the following general expressions for quadrupole sources of an axisymmetric turbulence

$$I_{1111}(\tau) = \rho^2 \frac{\partial^4}{\partial \tau^4} g^2(\tau) \frac{(\overline{u_1^2})^2 L_1^3 \Delta^2}{2\sqrt{2}}, \qquad (15a)$$

$$I_{2222} = I_{3333} = C_1 I_{1111},$$

$$I_{1122} = I_{1133} = C_2 I_{1111},$$

$$I_{2233} = C_3 I_{1111},$$

$$I_{1212} = I_{1313} = C_4 I_{1111},$$

$$I_{2323} = C_5 I_{1111},$$

where

$$C_1 = \frac{3}{2}\beta^2 + \frac{1}{32}[9(\Delta + \Delta^{-1})^4 - 48(\Delta + \Delta^{-1})^2 + 80]$$

$$-\frac{\beta}{4}(6 - \Delta^2 + 3\Delta^{-2}), \qquad (15b)$$

$$C_3 = \frac{1}{8}[\frac{3}{4}(\Delta + \Delta^{-1})^4 - 4(\Delta + \Delta^{-1})^2 + 7 - 2\Delta^2 + 4\beta^2$$

$$+2\beta(\Delta^2 - 2 - \Delta^{-2})],$$

$$C_2 = \frac{1}{8}, \quad C_4 = \frac{1}{16}(5 + 2\Delta^{-2} - 8\beta), \quad C_5 = \frac{1}{2}(C_1 - C_3),$$

and

$$\Delta = \frac{L_2}{L_1}, \qquad \beta = (1 - \frac{\overline{u_2^2}}{\overline{u_1^2}}). \qquad (16)$$

In the limiting case of an isotropic turbulence, $\Delta = 1$, $\beta = 0$, and coefficients $C_i \quad (i = 1, \cdots 5)$ reduce to those given by Eq. (7).

Equation (4) combined with (15a) gives spectral component $I_{1111}(\Omega)$. The integral length-scale $L_1$ is associated with turbulence kinetic energy and its dissipation rate $\epsilon$ (see Ref. 11) as

$$L_1 = \alpha_1 (\overline{u_1^2})^{3/2}/\epsilon, \qquad \epsilon = \nu \overline{(\partial u_i/\partial x_j)(\partial u_i/\partial x_j)}, \quad (17)$$

where $\alpha_1$ is an empirical constant. Similarly, the turbulence characteristic frequency $\Omega_o$, which is the inverse of the characteristic time-delay $\tau_o$, relates to $k$ and $\epsilon$

$$\tau_o = \frac{1}{\Omega_o} = \alpha_2 \frac{k}{\epsilon}, \qquad (18)$$

where $\alpha_2$ is a proportionality constant. From (17) and (18), we find that the longitudinal length-scale is inversely proportional to the characteristic source frequency

$$L_1 = (\frac{\alpha_1}{\alpha_2}) \frac{k^{0.5}}{\Omega_o} (\frac{3}{2} - \beta)^{-3/2}. \qquad (19)$$

The Transverse integral length-scale $L_2$ may be written similarly as $L_2 \sim (\overline{u_2^2})^{3/2}/\epsilon$; however, in the present study, we specify the ratio of length-scales as an arbitrary parameter $\Delta$ and write $L_2 = L_1 \Delta$. Using Eqs. (9) and (19) in (15a), it follows that

$$I_{1111}(\tau) = (\frac{\alpha_1}{\alpha_2})^3 \frac{\sqrt{2}}{4} \rho^2 \frac{\partial^4}{\partial \tau^4} g^2(\tau) k^{7/2} \tau_o^3 \Delta^2 (\frac{3}{2} - \beta)^{-13/2}. \qquad (20)$$

### 2.3 Non-Separable Two-Point Correlations

We now demonstrate that space and time separation is not a requirement for modeling the source functions. Indeed, similar results may be obtained with non-separable correlations. As indicated earlier, a two-point velocity correlation of an isotropic turbulence as defined in Eq. (5) is separable in space and time. For axisymmetric turbulence, the question of separability depends on selecting scalar functions $Q_1$ and $Q_2$. A simple inspection of Eq. (14) shows that these functions result in factorable correlations. For example, the axial two-point correlation is

$$\overline{v_1 v_1'} = -(2 + \xi_2 \frac{\partial}{\partial \xi_2} + \xi_3 \frac{\partial}{\partial \xi_3}) Q_1, \qquad (21)$$

which after a substitution of (14a) gives

$$\overline{v_1 v_1'} = \overline{u_1^2} \{1 - \pi \frac{\xi_{23}^2}{L_2^2}\} g(\tau) e^{-\pi(\xi_1^2/L_1^2 + \xi_{23}^2/L_2^2)}. \qquad (22)$$

This expression is factorable in variables $\vec{\xi}$ and $\tau$.

Now, let's consider a new set of kinematically acceptable scalar functions leading to non-separable correlations.

$$Q_1 = -(\frac{\overline{u_1^2}}{2}) e^{-\pi h(\tau)(\xi_1^2/L_1^2 + \xi_{23}^2/L_2^2)}, \qquad (23a)$$

$$Q_2 = -(\overline{u_2^2} - \overline{u_1^2}) e^{-\pi h(\tau)(\xi_1^2/L_1^2 + \xi_{23}^2/L_2^2)}. \qquad (23b)$$

From (23a) and (21) we have

$$\overline{v_1 v_1'} = \overline{u_1^2} \{1 - \pi h(\tau) \frac{\xi_{23}^2}{L_2^2}\} e^{-\pi h(\tau)(\xi_1^2/L_1^2 + \xi_{23}^2/L_2^2)}. \qquad (24)$$

This expression is clearly not factorable in space and time. A substitution of (24) in (3) gives the axial quadrupole source

$$I_{1111}(\tau) = \rho^2 \frac{\partial^4}{\partial \tau^4} \{h^{-3/2}(\tau)\} \frac{(\overline{u_1^2})^2 L_1^3 \Delta^2}{2\sqrt{2}}. \qquad (25)$$

Other source terms relate to $I_{1111}$ through coefficients $C_i$ exactly as given in (15b). Now, comparing (15a) and (25), we can conclude that two sets of scalar functions, (14) and (23), integrate to an identical source if $h(\tau) = g^{-4/3}(\tau)$. Similar arguments apply to the special case of an isotropic turbulence.
This example illustrates that 1) the separability assumption is simply a more convenient way of integrating the source correlation terms and 2) other non-separable functions may integrate to identical results.

### 3. Noise Sources and Mean-Flow Effects

We assume that the mean flow is parallel and that local density and sound speed are functions of radial coordinate $r$ only

$$U = U(r), \qquad \rho = \rho(r), \qquad a = a(r). \tag{26}$$

Lilley's equation for an inviscid flow linearized about a unidirectional transversely sheared mean flow is

$$\begin{aligned} L(p;U,x) &= \frac{1}{a^2}D^3p - D\nabla^2 p - \frac{d}{dr}(loga^2)D\frac{\partial p}{\partial r} + 2\frac{dU}{dr}\frac{\partial^2 p}{\partial x \partial r} \\ &= \rho D\frac{\partial^2}{\partial x_i \partial x_j}(v_i v_j) - 2\rho\frac{dU}{dr}\frac{\partial^2}{\partial x_1 \partial x_j}(v_2 v_j) + \cdots, \end{aligned} \tag{27}$$

where $r, \phi, x$ denote the cylindrical coordinates, $D$ is convective derivative $D = \frac{\partial}{\partial t} + U\frac{\partial}{\partial x}$, and $\nabla^2$ is the Laplacian operator in a cylindrical coordinate system.

The terms on the right hand side of (27) are the self- and the shear-noise source terms, respectively. Additional sources appear on the right hand-side of this equation as a result of the linearization process. Reference 12 argues that the remainder source terms (together) produce a negligible acoustic field. Using a direct numerical simulation (DNS) of the unsteady Navier-Stokes equation, Colonius *et al*[12] compute the acoustic field due to a plane mixing layer and compare that result with acoustic predictions from Lilley's equations. Their DNS calculations agree quite well with predictions of Lilley's equation using simplified sources, i.e. self- and shear-noise terms.

To account for refraction due to interaction of the mean flow with radiated sound, Balsa[13] worked out a high-frequency Green's function for the axisymmetric Lilley's equation. Refraction in non-axisymmetric jets can be studied in the high frequency limit using methods of geometric acoustics[14]. Ray-acoustics, however, is computationally intensive and may not be a very practical approach when dealing with complex geometries.

Here we employ Balsa's solution and write the Green's function $G$ for a monopole source convecting downstream with convection velocity $U_c$,

$$L(G;U,x) = e^{-i\Omega t}\delta(x - U_c t)\delta(r - r_o)\delta(\phi - \phi_o)/r, \tag{28}$$

where subscript $o$ refers to source location and $\Omega$ denotes source frequency. Let $S_1$ and $S_2$ be the Green's functions to the following equations, which correspond to self- and shear-noise terms of Lilley's equation,

$$L(S_1;U,x) = \rho D\{e^{-i\Omega t}\delta(x - U_c t)\delta(r - r_o)\delta(\phi - \phi_o)/r\}, \tag{29}$$

$$L(S_2;U,x) = -2\rho e^{-i\Omega t}\frac{dU}{dr}\delta(x - U_c t)\delta(r - r_o)\delta(\phi - \phi_o)/r. \tag{30}$$

It is easily shown that

$$S_1 = -i\rho\Omega\left(\frac{1 - M_o cos\theta}{1 - M_c cos\theta}\right)G, \tag{31}$$

where $M_o = U/a_\infty$ and $M_c = U_c/a_\infty$ and $\theta$ is the polar observer angle with respect to downstream jet axis. Similarly, neglecting higher order derivatives of the mean velocity in the operator part of Lilley's equation, i.e. $d^n U/dr^n = 0$ for $(n \geq 2)$, we obtain

$$S_2 = (-2\rho\frac{dU}{dr})G. \tag{32}$$

In deriving (31) and (32), we neglect the density gradient $d\rho/dr$. Transverse gradients of the mean density produce additional sources of monopole and dipole type as discussed by Mani[15]. From (31) and (32), the Green's functions for the two source types are related

$$S_2 = \left(\frac{2dU/dr}{i\Omega}\,\frac{1 - M_c cos\theta}{1 - M_o cos\theta}\right)S_1. \tag{33}$$

Appropriate double derivatives of the $S_1$ and $S_2$ with respect to source coordinates $x_i$ result in directivity factors due to quadrupole sources of self- and shear-noise

$$\mathcal{D}_{ij}^{\ell} = \frac{\partial^2 S_\ell}{\partial x_i \partial x_j}, \qquad (\ell = 1, 2). \tag{34a}$$

Next, the magnitude of $\mathcal{D}_{ij}$ is averaged circumferentially with respect to $\phi$ and $\phi_o$. For self-noise ($\ell = 1$) it follows that

$$a_{ij} = \frac{1}{4\pi^2}\int_{-\pi}^{+\pi} d\phi_o \int_{-\pi}^{+\pi} d\phi \mid \mathcal{D}_{ij}^1 \mid^2. \tag{34b}$$

A listing of quadrupole directivity factors $a_{ij}$ associated with self-noise terms of different orientation are provided in the Appendix. Directivity factors $b_{ij}$ for shear-noise are

$$b_{ij} = \left(\frac{2dU/dr}{\Omega}\,\frac{1 - M_c cos\theta}{1 - M_o cos\theta}\right)^2 a_{ij}. \tag{35}$$

In the far-field, mean-square sound pressure may be considered a superposition of mean-square acoustic radiation from independent correlation volume elements

within the jet. A unit volume of turbulence will contribute to self-noise as

$$\sum(\text{Self}-\text{noise}) = I_{1111}a_{11}+I_{2222}a_{22}+I_{3333}a_{33}+2(I_{1122}+2I_{1212})a_{12}+2(I_{1133}+2I_{1313})a_{13}+2(I_{2233}+2I_{2323})a_{23}. \quad (36)$$

For axisymmetric jets, $a_{22} = a_{33}$ and $a_{12} = a_{13}$, and (36) simplifies

$$\sum(\text{Self}-\text{noise}) = I_{1111}\{a_{11} + 2C_1a_{22} + 4(C_2 + 2C_4)a_{12} +2(C_3 + 2C_5)a_{yz}\}. \quad (37)$$

Similarly, for shear-noise, we have

$$\sum(\text{Shear}-\text{noise}) = b_{11}I_{2121}+b_{12}I_{2222}+b_{13}I_{2323}, \quad (38a)$$

or

$$\sum(\text{Shear}-\text{noise}) = I_{1111}\{C_4b_{11}+(C_1+C_5)b_{12}\}. \quad (38b)$$

Combining common factors from directivity elements $a_{ij}$ with source term $I_{1111}$, and keeping notation $a_{ij}$ to represent new directivity factors, power spectral directivity of an axisymmetric jet is expressed as

$$\overline{p^2_{\text{Self}}}(R,\theta,\Omega) \sim \int_{\vec{y}}\int_{-\infty}^{+\infty} \Lambda_1\{a_{11} + 2C_1a_{22} + 4(C_2 +2C_4)a_{12} + 2(C_3 + 2C_5)a_{23}\}e^{i\Omega\tau}d\tau d\vec{y}, \quad (39a)$$

$$\overline{p^2_{\text{Shear}}}(R,\theta,\Omega) \sim \int_{\vec{y}}\int_{-\infty}^{+\infty} \Lambda_2\{C_4a_{11} + (C_1 +C_5)a_{12}\}e^{i\Omega\tau}d\tau d\vec{y}, \quad (39b)$$

where

$$\Lambda_1 = \frac{(\frac{\rho_\infty}{\rho})^2 I_{1111}(\tau)}{(4\pi Raa_\infty)^2(1-M_ocos\theta)^2(1-M_ccos\theta)^2}, \quad (40a)$$

$$\Lambda_2 = (\frac{2dU/dr}{\Omega}\,\frac{1-M_ccos\theta}{1-M_ocos\theta})^2\Lambda_1. \quad (40b)$$

To proceed with integration on $\tau$, we notice

$$\int_{-\infty}^{+\infty}\frac{\partial^4}{\partial\tau^4}g^2(\tau)e^{i\Omega\tau}d\tau = \Omega^4\int_{-\infty}^{+\infty} g^2(\tau)e^{i\Omega\tau}d\tau. \quad (41)$$

Various time-delay functions were attempted. Here we assume $g(\tau) = exp(-\sqrt{(\sigma/2)^2+(\tau/\tau_o)^2})$ where $\sigma$ is an empirical constant ($\sigma \sim 0.80$) and $\tau_o$ is defined in (18). A normalizing factor of $exp(\sigma/2)$ is dropped from $g(\tau)$ as it multiplies other constants. The present form of $g(\tau)$ provides an overall improvement in predicted spectra at high frequencies compared to a Guassian function $g(\tau) = exp(-\tau^2/\tau_o^2)$ used in Ref. 11. Hence

$$g(\tau) = e^{-\sqrt{(\sigma/2)^2+(\tau/\tau_o)^2}},$$

$$\int_{-\infty}^{+\infty} g^2(\tau)e^{i\Omega\tau}d\tau = \sigma\tau_o\frac{K_1(\sigma\sqrt{1+(\Omega\tau_o/2)^2})}{\sqrt{1+(\Omega\tau_o/2)^2}}, \quad (42)$$

where $K_1$ is a modified Bessel function of the second kind and of order one. Then from (20), (41), and (42), the spectral density for the axial quadrupole source component becomes

$$I_{1111}(\Omega) \sim \rho^2k^{7/2}(\Omega\tau_o)^4\frac{K_1(\sigma\sqrt{1+(\Omega\tau_o/2)^2})}{\sqrt{1+(\Omega\tau_o/2)^2}}\times \Delta^2\left(1-\frac{2}{3}\beta\right)^{-13/2}. \quad (43)$$

Source and observer frequencies are related through a modified convection factor

$$\Omega = \omega\sqrt{(1-M_ccos\theta)^2+(\alpha_ck^{0.5}/a_\infty)^2}. \quad (44)$$

The empirical convection constant $\alpha_c$ was determined from comparison of predicted spectra with data.

Finally, Eq. (39), in conjunction with (40) and (43), is integrated over the jet plume. The final expressions for self- and shear-noise will depend on a pair of empirical proportionality factors. These calibration constants must be determined from sample noise measurements. We use the fact that shear-noise, as defined in (39b), has zero contribution at $\theta = 90^o$ (see expressions for $a_{11}$ and $a_{12}$ in the Appendix) and determine the constant factor multiplying self-noise. Near the downstream jet axis, on the other hand, shear-noise appears to peak. Contributions due to combined sources are matched with peak noise level near jet axis to determine the second constant.

## 4. Numerical Results

Flow field and acoustic predictions are presented here with emphasis on noise prediction and study of anisotropy parameters. Nozzle geometry consists of an axisymmetric dualstream flowfield (Fig. 2a) with a hot primary core ($T_{op} = 1442^oR$) and a cold bypass flow ($T_{ob} = 542^oR$) separated from the core by a "splitter" surface. Acoustic data was taken at an ambient Mach number of ($M_\infty = 0.27$) to simulate takeoff conditions. Flow measurements were taken at a lower freestream Mach number of ($M_\infty = 0.10$) due to excessive vibration of the LDV system. Table 1 describes the total pressure setting for the primary, bypass, and freestream for above test conditions. Flow computations were performed at both freestream conditions to validate flow as well as acoustic predictions.

Mean flow calculations were performed with the NPARC[16] Navier-Stokes solver and Chien's[17] $k$-$\epsilon$ turbulence model. The computational grid (Fig. 2b) starts at about 3 diameters upstream of the nozzle exit and extends to nearly 17 diameters from exit plane. In the radial direction, the external flowfield boundary conditions are specified at 17 diameters from centerline. Figure 3 shows predicted flow profiles for mean velocity and turbulence kinetic energy at ($M_\infty = 0.10$). Although more data at larger values of $X/D$ would be highly desirable, the predictions seem to capture the general trend, and in particular the maximum level of turbulence near the lipline at ($X/D = 4.0$) is close to measurement of Zysman*et al*[3]. Centerline values for the above parameters (Fig. 4) show a relatively high level of turbulence at the end of the computational grid. No measurements were available for validation beyond (X/D=4.0).

**Table 1**

| $M_\infty$ | $P_{op}$ | $P_{ob}$ | $P_{o\infty}$ |
|---|---|---|---|
| 0.10 | 28.02 | 26.43 | 14.31 |
| 0.27 | 28.81 | 26.13 | 15.10 |

Noise predictions are based on plume integration of expressions (39a) and (39b), starting from the nozzle exit plane. Additional high frequency noise may be generated within the nozzle due to primary and bypass jets mixing prior to exit plane. These considerations were not accounted for in the current predictions. The overall sound pressure level directivity due to self- and shear-noise sources as well as total directivity of the mixing noise are shown in Figure 5. At $90^o$, self-noise is the only contributing source, while shear-noise appears to peak near the downstream jet axis. As indicated earlier, two unknown calibration constants for expressions (39a) and (39b) were determined from acoustic measurements at $90^o$ and $150^o$.

Spectral distribution (Fig. 6) indicates a dominance by shear-noise in the low-frequency regime and in a downstream direction. Anisotropy parameters $\Delta$ and $\overline{u_2^2}/\overline{u_1^2}$ were selected as 0.50 and 0.60, respectively. A deficiency in the high-frequency noise is noticed with decreasing observer angle $\theta$. One possible explanation may be complete neglect of the internal noise sources in present predictions. In addition, simplifications such as an assumption of constant density in the source terms of equation (27) may affect high-frequency noise. For hot jets, additional sources of dipole and monopole type related to $d\rho/dr$ and $d^2\rho/dr^2$ will appear in modeling of self- and shear-noise terms of Lilley's equation. These sources can be accounted for in a similar fashion if one assumes that singularities of various orders contribute independently to total acoustic intensity.

The significance of non-isotropy parameters $\Delta$ and $\overline{u_2^2}/\overline{u_1^2}$ was studied by changing the above factors independently. Figure 7 shows that although reducing the length-scale ratio $\Delta = L_2/L_1$ decreases the noise intensity, reduction in the turbulence intensity ratio $\overline{u_2^2}/\overline{u_1^2}$ works the opposite way and dominates the overall trend. In general, an increase in acoustic intensity of both self- and shear-noise is noticed with increasing source anisotropy. Figure 8 shows the SPL directivity of the total noise for the indicated range of anisotropy parameters. These observations point to a delicate sensitivity between jet noise and underlying turbulence characteristics. Although full non-isotropy is ideal, an axisymmetric turbulence may be accurate enough to model most jets of practical interest.

## 5. Concluding Remarks

We studied the impact of source anisotropy on aerodynamic mixing noise due to a fine-scale turbulence. An axisymmetric turbulence model was presented with the axis of symmetry aligned with jet axis. It was argued that space and time separation is not a requirement for modeling turbulence correlation functions and closed-form solutions for various fourth-order two-point space-time correlations were obtained. Source strength as well as time- and length-scales of noise generating turbulent eddies were linked to compressible Reynolds averaged Navier-Stokes solution with a $k$-$\epsilon$ turbulence model. Both self- and shear-noise terms of Lilley's equation were presented. Acoustic/flow interaction was accounted for as a solution to an axisymmetric Lilley's equation for a transversely sheared mean flow and in a high frequency limit.

Noise prediction and study of non-isotropy parameters were discussed for a Mach 1.0 dualflow jet. Predictions indicated an overall increase in noise level with increasing turbulence anisotropy. An increase in streamwise turbulent intensity relative to its span-wise components resulted in a higher noise level for both noise sources. We neglected density gradients in the current source modeling. It was suggested that a more rigorous analysis would find additional sources of dipole and monopole type associated with transverse density gradients.

Internal noise may also have a significant bearing on overall directivity and spectra specially when internal mixers are used. A complete prediction tool requires additional modules to address internal noise sources and their propagation and diffraction in the presence of nozzle boundaries.

## Acknowledgments

The authors would like to thank James DeBonis and Gary G. Podboy of NASA Lewis for their contributions to this work.

## References


[1]Jones, I. S. F., "Fluctuating Turbulent Stresses in the Noise-Producing Regions of a Circular Jet," *J. Fluid Mech.*, **36**, pp. 529-543, 1969.

[2]Bradshaw, P., Ferriss, D. H., and Johnson, R. F., "Turbulence in the Noise-Producing Regions of a Circular Jet," *J. Fluid Mech.*, **19**, pp. 591-624, 1964.

[3]Zysman, S. H., Chiappetta, L. M., Saiyed, N. H., and Podboy, G. G., "Flowfield Measurement and Analysis of a 1/7-Scale Mixed Flow Exhaust System Model," *AIAA* paper 95-2744, 1995.

[4]Podboy, G. G., Bridges, J. E., Saiyed, N. H., and Krupar, M. J., "Laser Doppler Velocimeter System for Subsonic Jet Mixer Nozzle Testing at the NASA Lewis Aeroacoustics Propulsion Lab," *AIAA* paper 95-2787, 1995.

[5]Chandrasekhar, S., "The Theory of Axisymmetric Turbulence," Philos. Trans. R. Soc. London, **A 242,** pp. 557-577, 1950.

[6]Batchelor, G. K. , "The Theory of Axisymmetric Turbulence," Proc. R. Soc. London, **A 186,** pp. 480-502, 1946.

[7]Batchelor, G. K. , "The Theory of Homogeneous Turbulence," (Cambridge U.P., Cambridge, England, 1960).

[8]Ribner, H. S., "Quadrupole Corrections Governing the Pattern of Jet Noise," *J. Fluid Mech.*, **38**, pp. 1-24, 1969.

[9]Goldstein, M. E. and Rosenbaum, B. M., "Effect of Anisotropic Turbulence on Aerodynamic Noise," *J. Acoust. Soc. Am.*, **54** (3), pp. 630-645, 1973.

[10]Bechara, W., Lafon, P., and Bailly C., "Application of a $k$-$\epsilon$ Turbulence Model to the Prediction of Noise for Simple and Coaxial Free Jets," *J. Acoust. Soc. Am.*, **97** (6), pp. 3518-3531, 1995.

[11]Khavaran, A., Krejsa, E. A., and Kim, C. M., "Computation of Supersonic Jet Mixing Noise for an Axisymmetric Convergent-Divergent Nozzle," *J. Aircraft*, **31** (3), 1994.

[12]Colonius, T., Lele, S. K., and Moin, P., "Sound Generation in a Mixing Layer," *J. Fluid Mech.*, **330**, pp. 375-409, 1997.

[13]Balsa, T. F., "The Far Field of High Frequency Convected Singularities in Sheared Flows, with an Application to Jet Noise Prediction," *J. Fluid Mech.*, **74**, pp. 193-208, 1976.

[14]Khavaran, A., "Refraction and Shielding of Noise in Non-Axisymmetric Jets," *AIAA* paper 96-1780, 1996.

[15]Mani, R., "The Influence of Jet Flow on Jet Noise, Part 2. The Noise of Heated Jets," *J. Fluid Mech.*, **73**, pp. 779-793, 1976.

[16]Cooper, G. K. and Sirbaugh, J. R., "PARC Code: Theory and Usage," Arnold Engineering Development Center Report AEDC-TR-89-15, December 1989.

[17]Chien, K. Y., "Predictions of Channel and Boundary-Layer Flows with a Low-Reynolds-Number Turbulence Model," *AIAA Journal* **20**(1), pp. 33-38, 1982.

[18]Mani, R., *et al*, "High Velocity Jet Noise Source Location and Reduction," Task 2, FAA-RD-76-79-II, 1978.


## Appendix

Directivity factors for various convecting quadrupole source components are (see Ref. 18)

$$a_{11} = \frac{cos^4\,\theta\,\beta_{11}}{(1 - M_c\,cos\,\theta)^4}, \qquad a_{12} = \frac{g_o^2\,cos^2\,\theta\,\beta_{12}}{2(1 - M_c\,cos\,\theta)^2},$$

$$a_{22} = \frac{3}{8}\,g_o^4\,\beta_{22}, \qquad a_{23} = \frac{1}{8}\,g_o^4\,\beta_{23}, \qquad (A1)$$

and $g_o^2$ is the value of the shielding function $g^2(r)$ at the source location $r_o$

$$g^2(r) = \frac{(1 - M_o cos\theta)^2(\frac{a_\infty}{a})^2 - cos^2\theta}{(1 - M_e cos\theta)^2}. \qquad (A2)$$

The location $r_\sigma$, where $g^2(r_\sigma)$ becomes zero, is referred to as a turning point. When $g^2$ becomes negative, a shielding zone exists. The amount of shielding depends upon the proximity of the source with respect to the turning point $r_\sigma$ as well as the number of turning points. This dependence is incorporated through shielding coefficients $\beta_{11}$, $\beta_{22}\,\cdots$. For example, when there is only one turning point $r_{\sigma 1}$, the shielding coefficients $\beta$ become constant multipliers of $exp(-2K\int_{r_o}^{r_{\sigma 1}}\sqrt{\mid g^2(r)\mid}dr)$ where $K = \Omega/a_\infty$. A complete listing of $\beta_{ij}$ for various source correlation elements and their dependence on the number of turning points is given in Ref. 18.

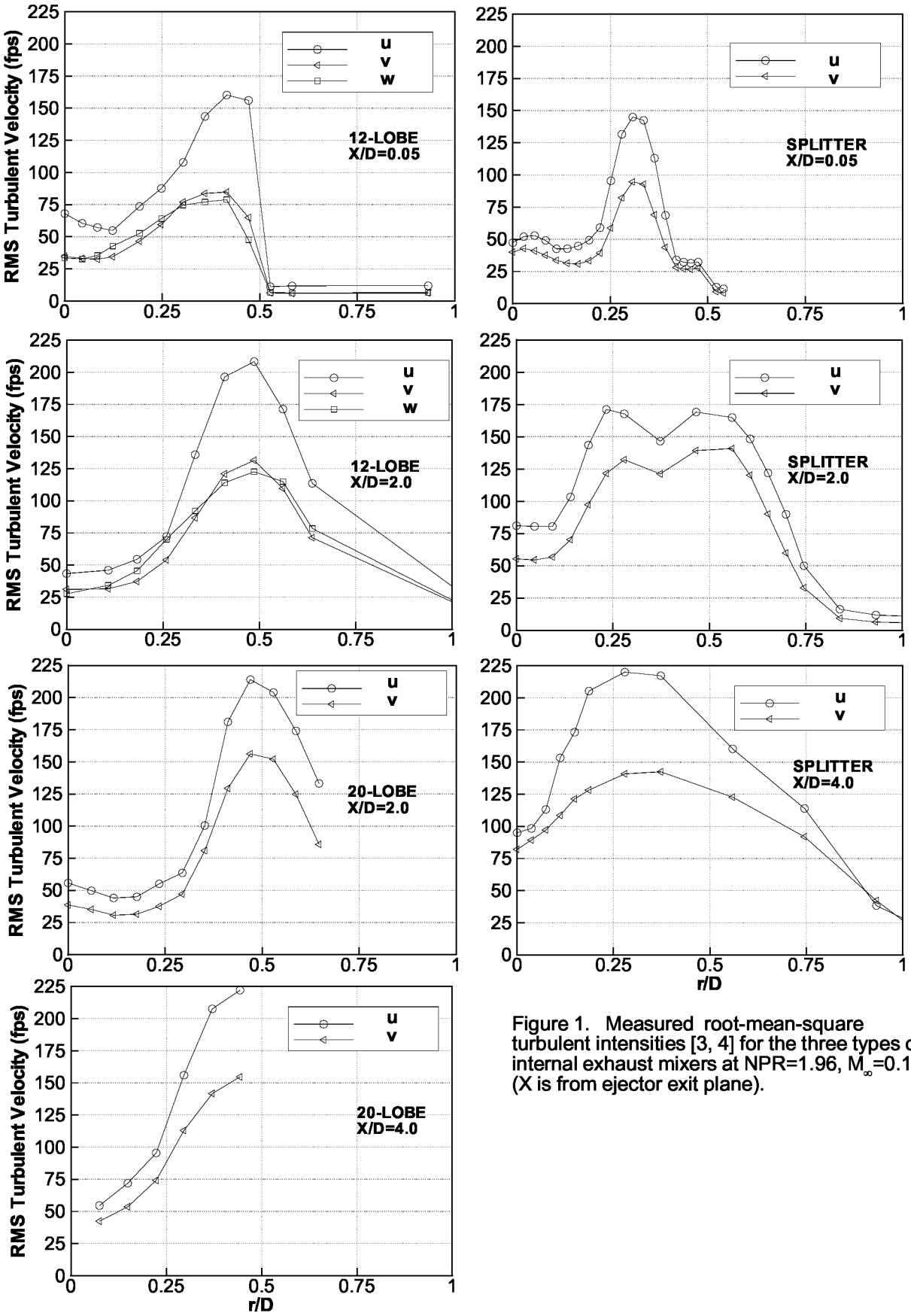


Figure 1. Measured root-mean-square turbulent intensities [3, 4] for the three types of internal exhaust mixers at NPR=1.96, $M_\infty$=0.10. (X is from ejector exit plane).

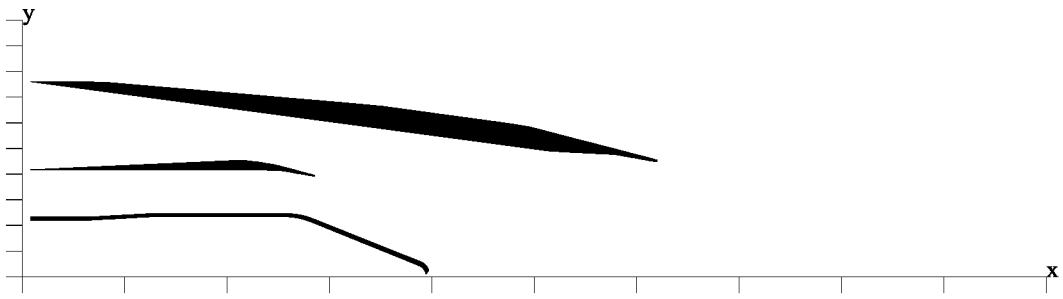


Figure 2a. Splitter nozzle geometry.

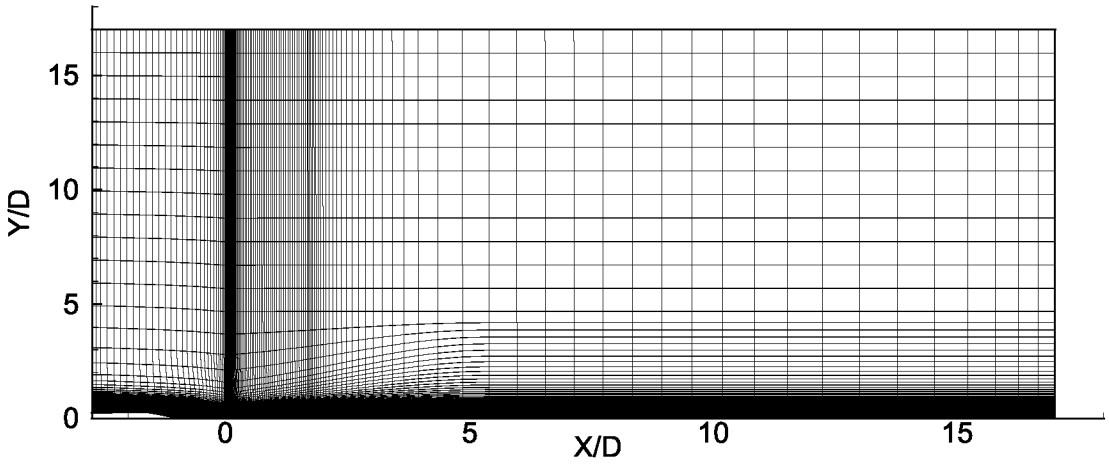


Figure 2b. Computational grid (400x133). X is from exit plane and D is nozzle exit diameter.

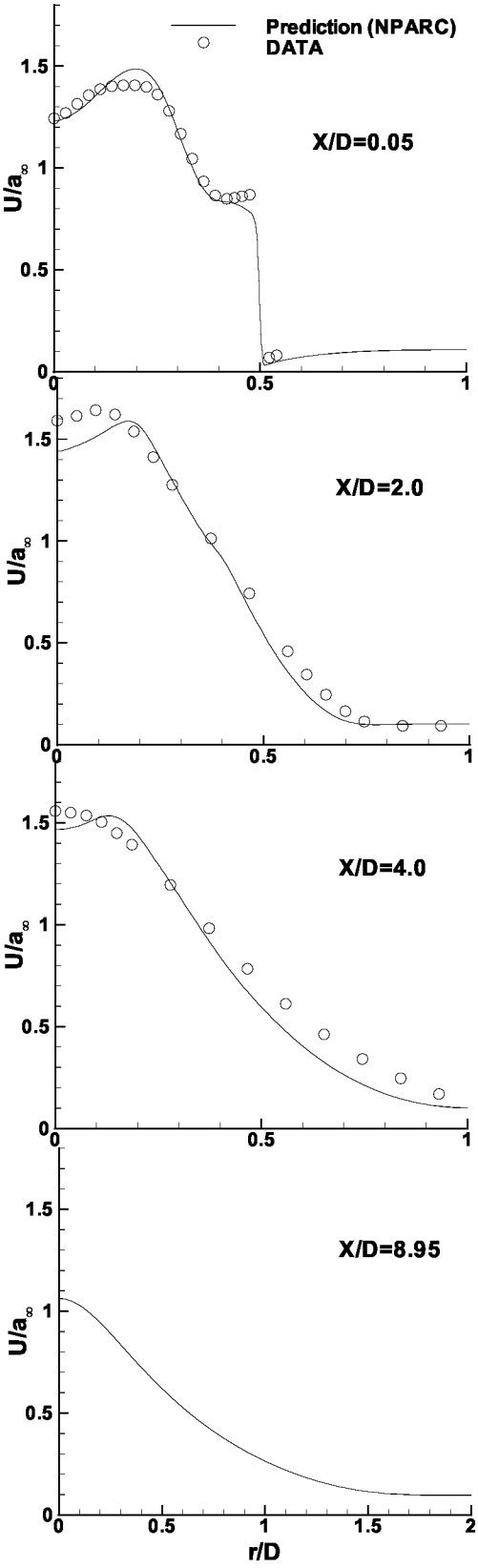


Figure 3a. Comparison of predicted and measured [3] axial velocity profiles for the Splitter nozzle (NPR=1.96, $M_\infty$=0.10 , T=1442° R).

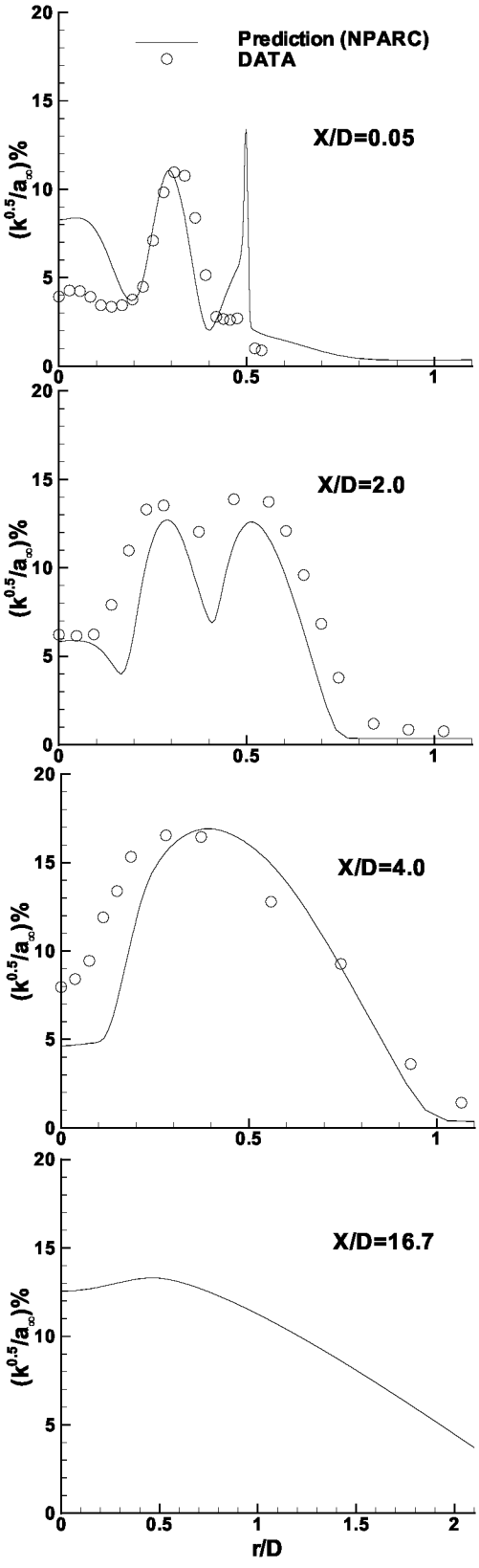


Figure 3b. Comparison of predicted and measured [3] turbulence kinetic energy profiles for the Splitter nozzle.

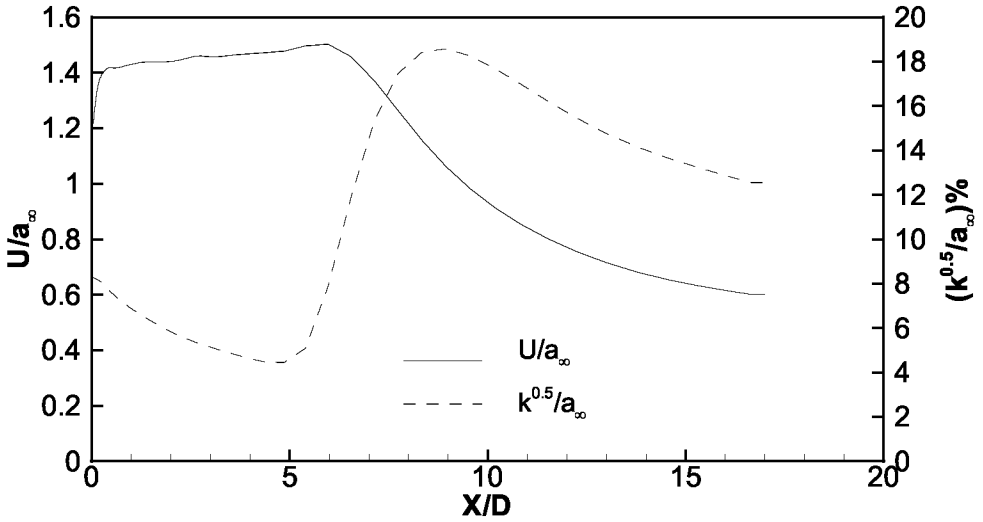


Figure 4. Predicted centerline values for mean velocity and turbulence kinetic energy (X is from nozzle exit plane).

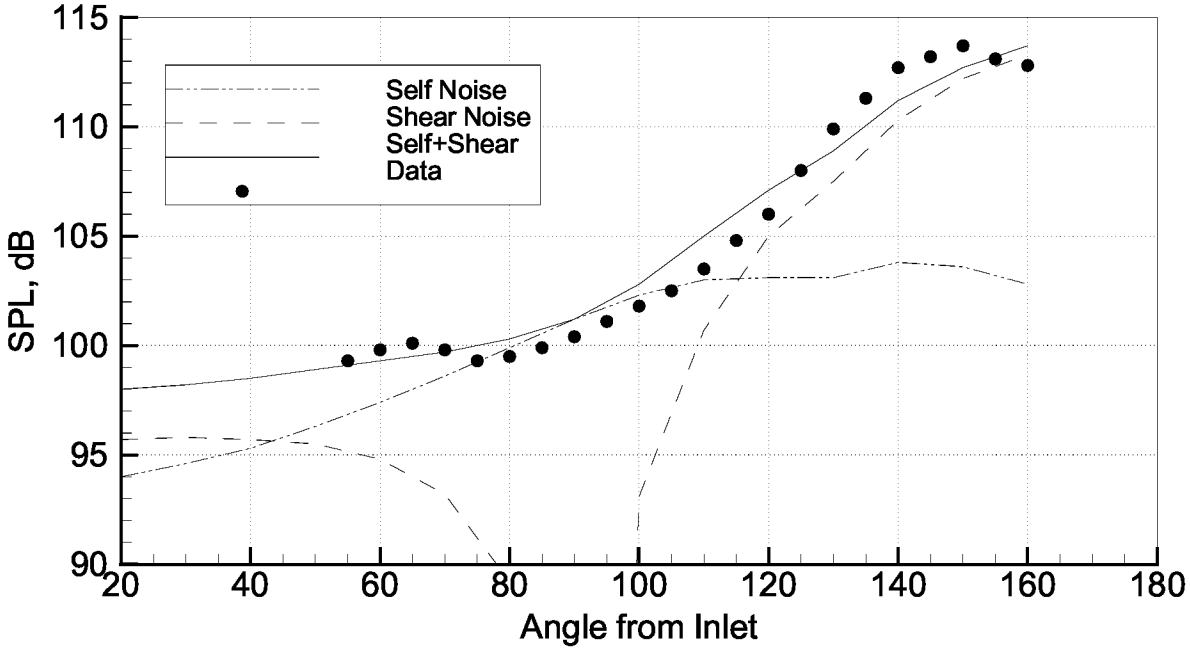


Figure 5. Sound pressure level directivity for the Splitter nozzle at NPR=1.96, T=1442°, $M_\infty$=0.27 and on a 50.0 ft. arc. Non-isotropy parameters are $\Delta$=0.50 and $u_2^2/u_1^2$=0.60.

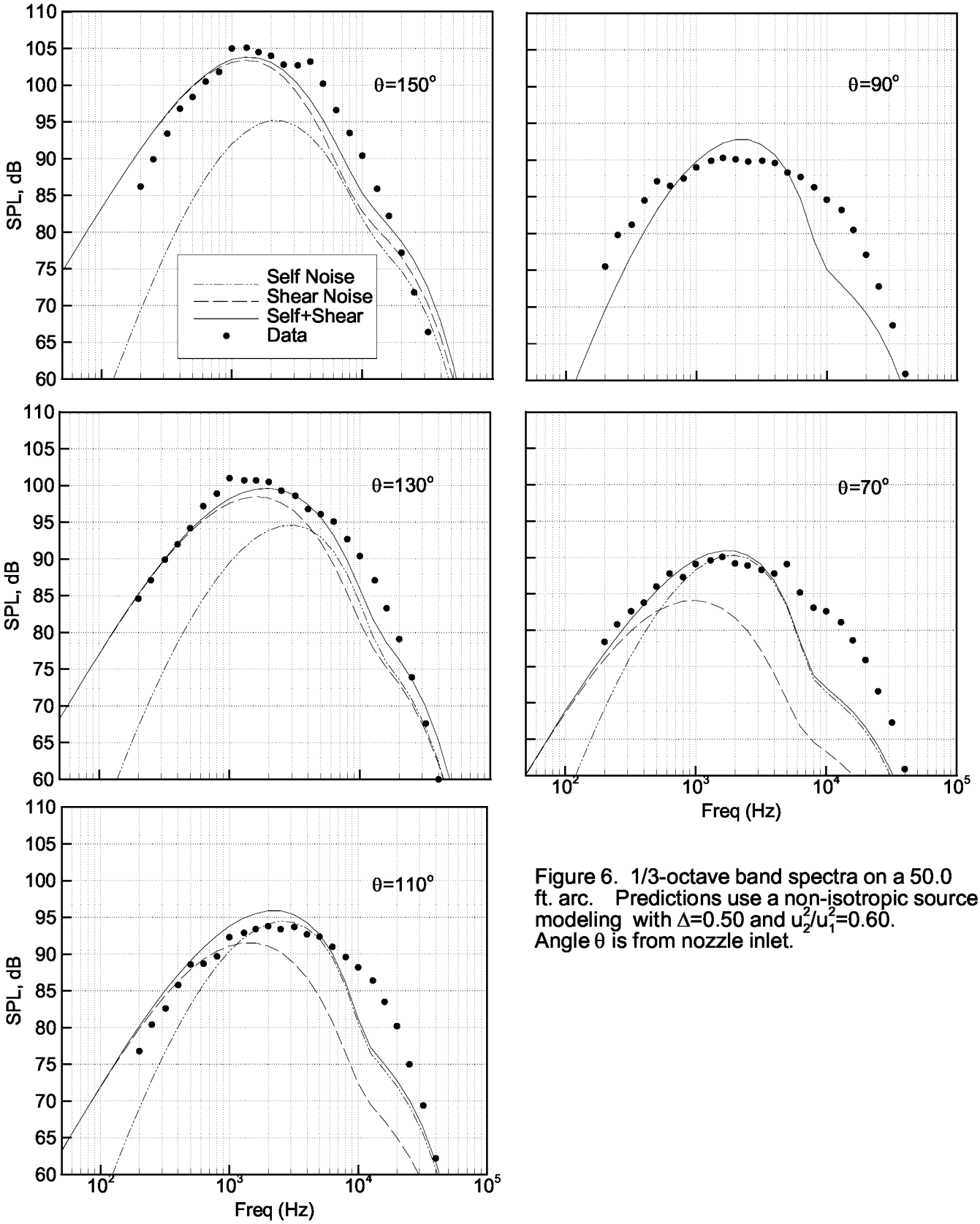


Figure 6. 1/3-octave band spectra on a 50.0 ft. arc. Predictions use a non-isotropic source modeling with $\Delta$=0.50 and $u_2^2/u_1^2$=0.60. Angle $\theta$ is from nozzle inlet.

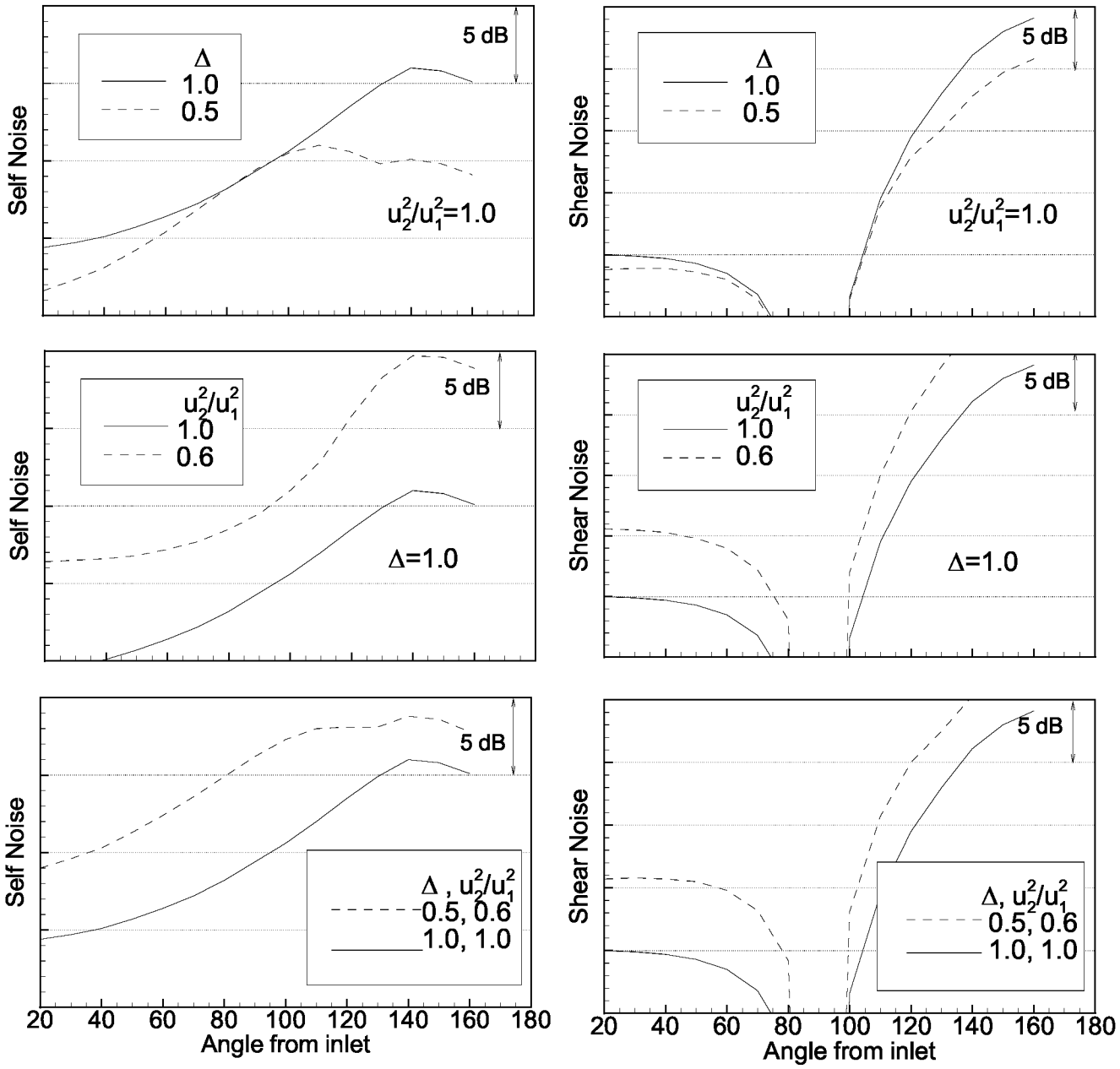


Figure 7. Sensitivity of self- and shear-noise components to non-isotrpy parameters Δ $u_2^2/u_1^2$ in an axisymmetric turbulence model. Predictions are for the Splitter nozzle and on arc=50.0 ft.

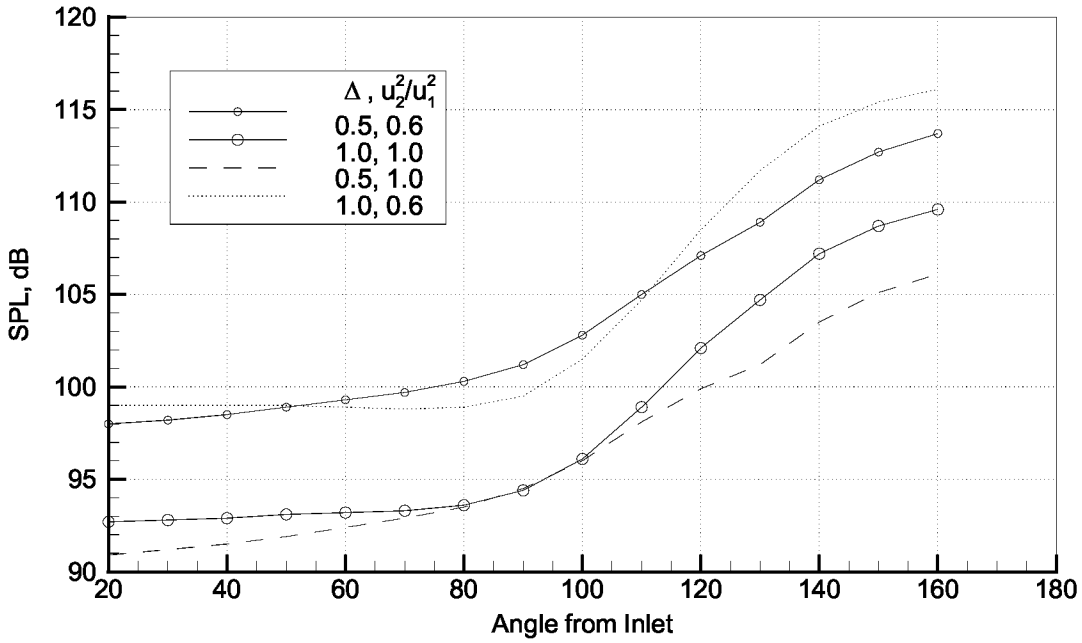


Figure 8. Sound pressure level directivity vs. non-isotropy parameters $\Delta$ and $u_2^2/u_1^2$.

# REPORT DOCUMENTATION PAGE

*Form Approved*
*OMB No. 0704-0188*



| 1. AGENCY USE ONLY (*Leave blank*) | 2. REPORT DATE | 3. REPORT TYPE AND DATES COVERED |
|---|---|---|
| | May 1998 | Technical Memorandum |

**4. TITLE AND SUBTITLE**

On the Role of Anisotropy in Turbulent Mixing Noise

**5. FUNDING NUMBERS**

WU–537–05–21–00

**6. AUTHOR(S)**

A. Khavaran and E.A. Krejsa

**7. PERFORMING ORGANIZATION NAME(S) AND ADDRESS(ES)**

National Aeronautics and Space Administration
Lewis Research Center
Cleveland, Ohio 44135–3191

**8. PERFORMING ORGANIZATION REPORT NUMBER**

E–11207

**9. SPONSORING/MONITORING AGENCY NAME(S) AND ADDRESS(ES)**

National Aeronautics and Space Administration
Washington, DC 20546–0001

**10. SPONSORING/MONITORING AGENCY REPORT NUMBER**

NASA TM—1998-207922
AIAA–98–2289

**11. SUPPLEMENTARY NOTES**

Prepared for the Fourth Aeroacoustics Conference cosponsored by the American Institute of Aeronautics and Astronautics and the Confederation of European Aerospace Societies, Toulouse, France, June 2–4, 1998. A. Khavaran, NYMA, Inc., 2001 Aerospace Parkway, Brook Park, Ohio 44142 (work performed under NASA Contract NAS3–27186); E.A. Krejsa, NASA Lewis Research Center. Responsible person, E.A. Krejsa, organization code 5940, (216) 433–3951.

**12a. DISTRIBUTION/AVAILABILITY STATEMENT**

Unclassified - Unlimited
Subject Categories: 07 and 71 Distribution: Nonstandard

This publication is available from the NASA Center for AeroSpace Information, (301) 621–0390.

**12b. DISTRIBUTION CODE**

**13. ABSTRACT** ***(Maximum 200 words)***

This paper investigates the effect of anisotropy on aerodynamic mixing noise due to a fine-scale turbulence. The usual assumption of isotropic turbulence is replaced with that of an axisymmetric turbulence. The analysis is based on source terms of Lilley's equation. In addition, acoustic-flow interaction is accounted for in terms of a high-frequency solution to the axisymmetric Lilley's equation. In the limiting case of isotropy, various source correlation terms derived here will simplify to those obtained with an isotropic turbulence model. A Reynolds averaged Navier-Stokes solution with a $k$-$\varepsilon$ turbulence model for a Mach 1.0 jet was used to make acoustic predictions. A parametric study of the turbulence scales indicates that anisotropy increases the peak noise level.

| 14. SUBJECT TERMS | 15. NUMBER OF PAGES |
|---|---|
| Acoustics; Jet noise; Noise | 20 |
| | 16. PRICE CODE |
| | A03 |

| 17. SECURITY CLASSIFICATION OF REPORT | 18. SECURITY CLASSIFICATION OF THIS PAGE | 19. SECURITY CLASSIFICATION OF ABSTRACT | 20. LIMITATION OF ABSTRACT |
|---|---|---|---|
| Unclassified | Unclassified | Unclassified | |